Characteristics of Microfluidic Paper-based Analytical Devices Fabricated by Four Different Methods

Takeshi KOMATSU,*1 Masatoshi MAEKI,*2 Akihiko ISHIDA,*2 Hirofumi TANI,*2 and Manabu TOKESHI*2,*3,*4,*5†

*1 *Graduate School of Chemical Sciences and Engineering, Hokkaido University, Kita 13 Nishi 8, Sapporo 060–8628, Japan*
*2 *Division of Applied Chemistry, Faculty of Engineering, Hokkaido University, Kita 13 Nishi 8, Sapporo 060–8628, Japan*
*3 *ImPACT Research Centre for Advanced Nanobiodevices, Nagoya University, Furo-cho, Chikusa, Nagoya 464–8603, Japan*
*4 *Innovative Research Centre for Preventive Medical Engineering, Nagoya University, Furo-cho, Chikusa, Nagoya 464–8603, Japan*
*5 *Institute of Innovation for Future Society, Nagoya University, Furo-cho, Chikusa, Nagoya 464–8603, Japan*

We report on the effects of fabrication methods, photolithography, wax printing, screen printing, and craft cutting, on selected properties of microfluidic paper-based analytical devices (μPADs): cost, fabrication precision, wicking rate, and analytical accuracy. Photolithography requires numerous fabrication steps, and an oxygen plasma treatment is necessary when using an aqueous solution. Although the boundary between the hydrophobic and hydrophilic areas in the μPAD is sharpest, the obtained K-scale intensity in measuring of protein concentrations is lower than those of the devices by other methods. Wax printing offers the simplest and fastest fabrication, although solution leakage measures should be taken to improve the wicking rate and to prevent cross-contamination. Screen printing also offers easy fabrication. The screen-printed μPAD has a good wicking performance and shows a high detection intensity. Craft cutting allows automated fabrication of many μPADs at once. The craft cut μPAD has the fastest wicking rate among the four μPADs due to bare cellulose fibers. We consider that the detection intensity of this μPAD can be raised by optimizing the evaporation rate.

Keywords Paper-based analytical devices, photolithography, wax printing, screen printing, craft cutting

(Received April 24, 2017; Accepted June 30, 2017; Published January 10, 2018)

Introduction

Microfluidic paper-based analytical devices (μPADs) have great advantages, such as low cost, being easy to mass produce, use, carry around, and disposal after use.[1] For these reasons, μPADs are to be popular alternative devices to conventional ones for food safety analysis,[2,3] environmental monitoring,[4,5] and point-of-care diagnosis.[6-9] μPADs have been fabricated by a variety of methods, including (1) photolithography,[10-12] (2) wax printing,[12-14] (3) inkjet printing,[15-18] (4) screen printing,[19-22] and (5) craft cutting.[23-25] The main advantages and disadvantages of each fabrication method may be summarized as follows.

Method (1): The apparatus for photolithography is expensive, procedures are complicated, and a long fabrication time is required in comparison with the other fabrication methods. However, photolithography can fabricate channel patterns with high resolution.[10-12] Methods (2), (3) and (4): These printing methods enable low cost and easy fabrication. Method (5): Craft cutting machines are inexpensive. However, it is difficult for them to create microchannels on a paper precisely.

The various parameters of fabricated μPADs, such as cost, wicking rate, and edge clarity, have also been reported, and the fabrication methods affect these parameters.[1,11,26,27] In addition, we previously demonstrated the effect of a paper substrate on the sensitivity of μPADs.[12,28] The suitable fabrication method should be selected according to the target analytes and types of paper substrate. Some articles[1,11,26,27] have compared the precision, cost, and ease of the fabrication methods of μPADs as summaries of experimental results from several research groups. However, the effect of fabrication method on the analytical properties of μPADs has not been well investigated.

Here we considered the effect of the fabrication method on the μPAD properties: cost, fabrication accuracy, wicking rate and analytical precision. We selected the fabrication methods of photolithography, wax printing, screen printing, and craft cutting, because these methods are widely used for μPAD fabrication and the characteristics, as well as the advantages and disadvantages, of the methods are significantly different. The evaluations of fabrication methods and the μPADs themselves provide valuable information for developing novel μPADs and the promise of μPADs with better performance features.

† To whom correspondence should be addressed.
E-mail: tokeshi@eng.hokudai.ac.jp

Table 1 Investigation of the effects of fabrication methods on the properties: cost, fabrication accuracy, wicking rate and analytical precision, of μPADs using four types of fabrication methods

	Photolithography	Wax printing	Screen printing	Craft cutting
Ease of fabrication	×	◎	◎	◎
Fabrication time	×	◎	○	○
Raw materials costs[a]	~$(US)7.11/device	~$(US)1.55/device	~$(US)0.0376/device	~$(US)1.82/device
Fabrication efficiency	4 devices/h	10 devices/h	54 devices/h	12 devices/h
Pattering precision	◎	×	○	◎
SEM observation	○	×	◎	◎
Wicking rate (TB)	0.724 mm/s	0.574 mm/s	0.853 mm/s	0.960 mm/s
Wicking rate (SPW)	0.831 mm/s	0.810 mm/s	1.37 mm/s	1.97 mm/s
Instrument costs	~$(US)100000	~$(US)3000	~$(US)3000	~$(US)300
Characteristics	Sharp designs can be created	Simple and fast fabrication	Easy fabrication	Automated fabrication of many devices at one time
	Plasma treatment is required	The leakage of solution should be prevented to improve the cross-contamination	The μPAD indicates good properties	The μPAD is the fastest wicking rate and evaporation

◎, Great result. ○, Good result. ×, Bad result. a. Raw material costs are not included a cost of the fabricating instrument.

Experimental

Reagents and chemicals

Whatman chromatography paper #1 was purchased from GE Healthcare Japan Co., Ltd. (200 × 200 mm, thickness = 0.18 mm, Tokyo, Japan) and used as a substrate for μPAD devices. SU-8 2010 photoresist and SU-8 developer were obtained from Microchem (Westborough, MA, USA). Isopropanol, used to remove unreacted SU-8 developer, was purchased from Wako Pure Chemical Industries, Ltd. (Osaka, Japan). Polydimethylsiloxane (PDMS, SILPOT 184 CAT), used as hydrophobic ink for screen printing, was purchased from Dow Corning Toray Co., Ltd. (Tokyo, Japan). For edge observations, a 1 mM phenolphthalein solution was prepared by dissolving phenolphthalein (special grade, Kanto Chemical Co., Inc., Tokyo, Japan) in ultrapure water (Millipore water purification system, 18 MΩ cm, Milli-Q, Millipore, Bedford, MA, USA) and added 0.1 mM NaOH. To measure the wicking rate, 9 mM bromothymol blue (Wako special grade, Wako Pure Chemical Industries) was prepared by dissolving in 95% ethanol. Albumin, from bovine serum (Wako 1st grade) was obtained from Wako Pure Chemical Industries and used with ultrapure water to prepare BSA standard solutions (0, 20, 40 and 60 μM). A citrate buffer solution (250 mM, pH 1.8) was prepared by mixing (41:8 v/v) of a 250 mM trisodium citrate dihydrate solution (special grade, Wako Pure Chemical Industries, Ltd.) and a 250 mM citric acid solution (special grade, Kishida Chemical Co., Ltd., Osaka, Japan). To measure the BSA concentration, 9 mM tetrabromophenol blue (TBPB, Sigma-Aldrich Co., Inc.) was prepared by dissolving in 95% ethanol.

Pattern designs and fabrication procedures of μPADs

The patterns of the photomasks for photolithography were designed using AutoCAD 2015 (Autodesk, Inc., CA, USA), and then obtained from Unno Giken Co., Ltd. (Tokyo, Japan). The pattern of the hydrophobic barrier for the μPAD was designed using Inkscape and Adobe Illustrator (Adobe Systems Inc., Tokyo, Japan), for wax- and screen-printing methods, respectively. The pattern for the craft cut μPAD was designed using Silhouette Studio software (GRAPHTEC Corp., Kanagawa, Japan). As shown in Fig. S1 (Supporting Information), the channel design of the μPAD had eight channels connected to eight separate detection zones (ϕ = 4 mm) located around the buffer introduction zone (ϕ = 12 mm). The μPADs were fabricated by photolithography and screen printing, as described in our previous reports.[12,19,28,29] The μPADs were also fabricated by a wax printer (Xerox Tektronix PHASER 850, Xerox Corp., Tokyo, Japan) and a commercially available craft cutting machine (Silhouette CAMEO, GRAPHTEC Corp.), for a wax printing method and a cutting method, respectively. The detailed fabrication procedures are described in Supporting Information.

Protein assay procedure

First, 15 μL of a 250 mM citrate buffer solution (pH 1.8) was introduced into the buffer zone and was evaporated using a dryer for 2 min. Then, 15 μL of a 9 mM TBPB solution in 95% ethanol was introduced into the buffer zone and was evaporated using a dryer for 5 min. Finally, 3.5 μL of BSA solutions of different concentrations was separately spotted onto the eight detection zones. Colorimetry was used as the detection method. The distance between the μPAD and a digital camera (EOS Kiss X6i, Canon, Tokyo, Japan) was *ca.* 20 cm, and images of the PADs were taken using a digital camera under fluorescent lighting conditions. The color information was measured with an image analysis software program (ImageJ Ver. 1.48).

Results and Discussion

Evaluation of fabrication efficiency

In Table 1, we summarize our comparison of the μPADs fabricated by the four types of methods. First, we evaluated the ease of implementing each μPAD fabrication method. We fabricated the μPADs as shown in Fig. S2 (Supporting Information). Wax printing, screen printing, and craft cutting methods were very simple; especially, screen printing only required rubbing PDMS ink on the stencil several times using a squeegee to get ink penetration into the paper substrate. Wax printing and craft cutting could automatically fabricate μPADs using the respective apparatuses. However, photolithography included many fabrication steps and took a long time.

Then, we evaluated the fabrication throughput for the μPADs using each method. The fabrication efficiencies (as devices/fabrication at once) were 4, 12, 36, and 10, for photolithography, wax printing, screen printing, and craft cutting, respectively. Although the fabrication efficiency depends on the channel

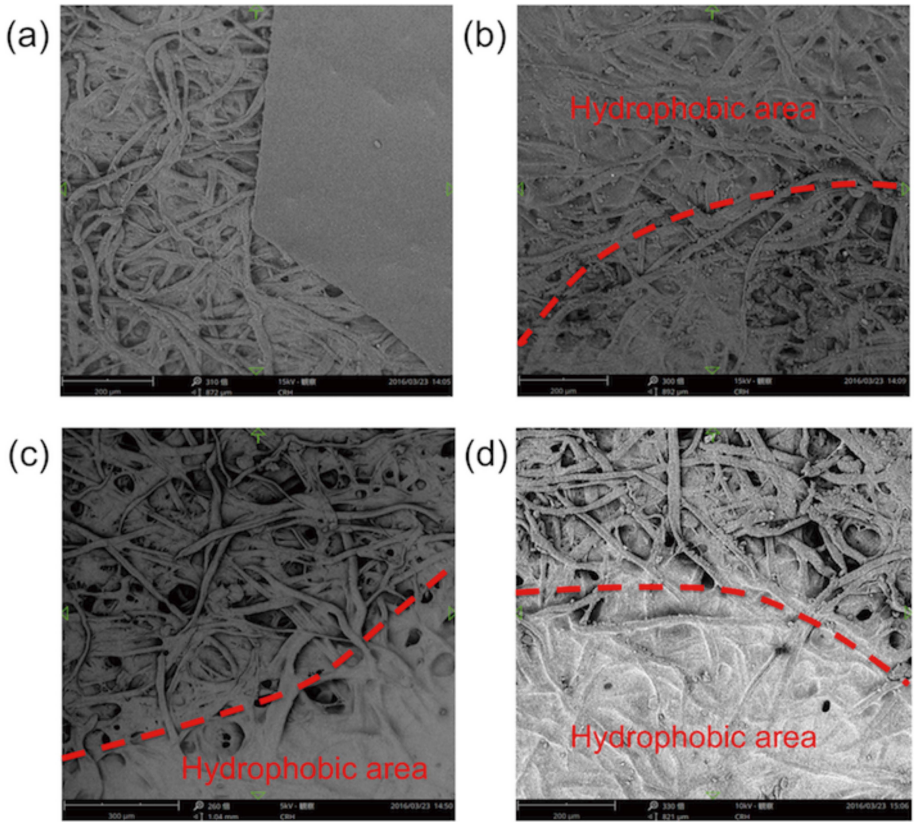

Fig. 1 Boundary between the hydrophobic area and the hydrophilic area of the μPAD (topside and backside) observed using a benchtop SEM. The left images (a, c) are the top side and the right images (b, d) are the back side of the μPAD. (a, b) show SEM images of the μPAD fabricated by photolithography and (c, d) show SEM images of the μPAD fabricated by screen printing.

pattern, screen printing had the highest fabricating efficiency among the four fabrication methods. We used a stencil with a 20-cm square printing area, and the μPAD size was 3-cm square. We were able to fabricate 36 μPADs at one time. The UV irradiation area of a typical mask aligner was 6 – 8 cm square. According to literature, we can assume the throughput of the number of fabricating μPADs (~2 cm square) to be 9 – 16 devices at one time.[10] Photolithography, in comparison, could fabricate only 4 μPADs at once due to the limited UV irradiation area (about an 8-cm square) and the size of the μPAD (about a 3-cm square). Wax printing and craft cutting had similar fabrication throughputs.

We also focused on the fabrication costs, calculated from the raw material costs, including the paper (Whatman chromatography paper #1: $40/100 papers) and reagents. The raw material costs were calculated as follows: Five milliliters of SU-8 2010 ($2290/L) and 200 mL of SU-8 developer ($85/L) were used for photolithography. Seven grams of PDMS ($0.136/g) were used for screen printing. The costs of the wax ink and cutting sheet were $36/color-ink and $12/sheet. From the material costs including the paper cost, we estimated the fabrication costs of μPADs. For photolithography, wax printing, screen printing, and craft cutting, the respective fabrication costs were estimated to be ~$7.11, ~$1.82, ~$0.0376, and ~$1.55, and the respective apparatus costs were ~$100000, ~$3000, ~$3000, and ~$300.

Evaluation of the patterning ability

We evaluated the patterning ability of each fabrication method. To prevent leakage of the solutions and contaminations, the hydrophobic and hydrophilic areas should be clearly patterned on the paper substrate. In this paper, we define the microchannel clearly patterned by hydrophobic ink as good channel patterning. Therefore, we observed the boundary between the hydrophobic area and hydrophilic area constituting the microchannel of the μPADs (topside and backside) using a benchtop SEM (proX PREMIUM, Phenom World Co., Ltd.). Figures 1(a) and 1(b) show SEM images of the μPAD fabricated by photolithography. The boundary between the hydrophobic and hydrophilic areas was clearly formed on the topside. However, it was not clearly formed on the backside of the μPAD. We assume that the photoresist could not completely crosslink due to poorer UV exposure on the paper backside. We can improve patterning of the channel design by using a thinner paper substrate or having an additional UV irradiation from the substrate backside. Figures 1(c) and 1(d) show SEM images of the μPAD fabricated by screen printing. For screen printing, the boundary between the hydrophobic and hydrophilic areas was clearly formed on both paper sides and the method showed the best channel patterning capability. The amount of PDMS ink can be adjusted depending on the paper substrate and channel design.[19] The optimal amount of PDMS ink and the rubbing frequency make it possible to fabricate μPADs with good channel patterning.

On the other hand, we did not confirm any significant difference between both sides of the μPADs fabricated by wax printing and craft cutting, as shown in Fig. S3 (a, b) (Supporting Information). The channel design of the μPAD fabricated by wax printing was clearly patterned as shown in Fig. S2

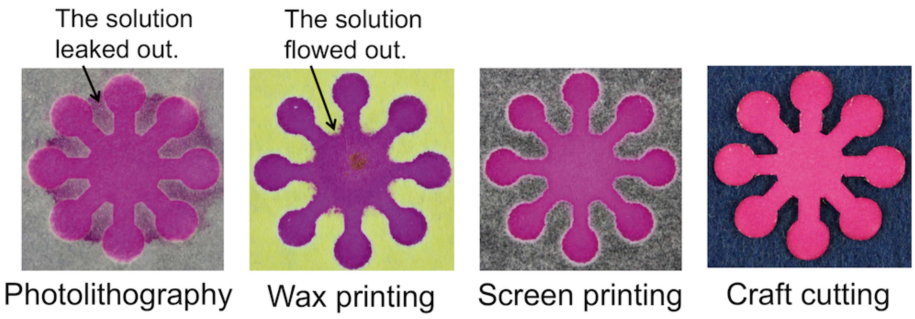

Fig. 2 Patterning precision evaluation using a 1 mM phenolphthalein solution for μPADs fabricated by the four methods.

(Supporting Information). However, the amount of printed wax ink was not enough to make the boundary between the hydrophobic and hydrophilic areas of the μPAD. For this reason, we consider that the wax ink could not penetrate uniformly into the cellulose fibers, and this might affect the performance of the μPAD. Wax printing can fabricate a completely patterned μPAD by controlling the melting point and heating time of the wax ink to prevent cross-contamination. In the case of craft cutting, all bare cellulose fibers were observed because it did not use chemicals (Fig. S3 (c, d)) (Supporting Information).

Then, a 1 mM phenolphthalein solution was pipetted onto each μPAD to observe the formed channel pattern. The μPAD fabricated by photolithography underwent an oxygen plasma treatment to increase the hydrophilicity. Figure 2 shows photographs of μPADs when the phenolphthalein solution was introduced. In the case of wax printing, the phenolphthalein solution flowed out from the buffer introduction zone. We think that the wax printed μPAD did not form a complete hydrophobic barrier (Fig. S3 (a, b)) (Supporting Information) due to insufficient wax ink on the paper substrate. In the case of photolithography, phenolphthalein solution did not fill every part of the μPAD and there was slight leakage out to the hydrophobic area. This result indicates the hydrophilicity of the whole μPAD (the extent of the hydrophobic and hydrophilic areas) was increased by the oxygen plasma treatment and it led to a penetration of the phenolphthalein solution into the hydrophobic area. In the case of craft cutting, we did not observe any leakage of the phenolphthalein solution from the buffer introduction zone of the μPAD put on pinholders, because the craft cut μPAD had only the hydrophilic area based on the presence of bare cellulose fibers. From these results, we conclude that the photolithography method can produce the most sharp channel among the four methods, although the fabrication methods would affect the performance of the μPADs, including their wicking rate, sensitivity, and precision of analysis. In the next section, we therefore evaluate the wicking rate of the μPADs.

Evaluation of the wicking rate

To evaluate the wicking rate changing of four fabrication methods, we measured the wicking rate of the μPADs using 9 mM bromothymol blue (dissolved in 95% ethanol). First, 15 μL of 9 mM bromothymol blue or ultrapure water was dropped onto the center part of the buffer introduction zone. Then, we measured the time for the solution to reach the detection zone. The wicking rates of bromothymol blue were 0.724 (RSD = 3.41%), 0.574 (6.23%), 0.853 (1.92%), and 0.960 (2.72%) mm/s, for photolithography, wax printing, screen printing, and craft cutting, respectively (see Table 1). The wicking rates of the μPADs fabricated by craft cutting and screen printing were faster than the other fabrication methods, because the channel areas were completely formed without any chemical processing. Contrary to our expectation, the μPAD fabricated by photolithography had a moderate wicking rate. For this experiment, because the μPAD had not undergone the oxygen plasma treatment, we consider that the organic solvent remained in the cellulose fibers, which promoted wicking of the ethanol-based solution. The μPAD fabricated by wax printing had the slowest wicking rate due to unclear patterning of the channel design.

We also measured the wicking rate under the same experimental procedures using ultrapure water. Water dropped onto the μPAD fabricated by photolithography without oxygen plasma treatment did not flow into the μPAD (Fig. S4). We then used the μPAD that had undergone the oxygen plasma treatment and measured the wicking rate of ultrapure water (Table 1). The wicking rates were 0.831 (RSD = 9.65%), 0.810 (12.8%), 1.37 (12.9%), and 1.97 (5.04%) mm/s, for photolithography, wax printing, screen printing, and craft cutting, respectively. Product information of Whatman chromatography paper #1 (thickness: 0.18 mm, weight: 87 g/m^2) is reported to be 130 mm/30 min (0.0722 mm/s). However, the provided wicking rate was measured by a different evaluation method from our case. We assume that the wicking rate of the μPAD fabricated by craft cutting shows a similar value with typical chromatography paper, because the μPAD is composed by bare cellulose fiber. Therefore, we compared the wicking rate of the craft cutting device and other devices. The wicking rates of the μPADs fabricated by craft cutting and screen printing were also faster than the other fabrication methods, because the channel area were completely formed without any chemical processing. The hydrophilicity of the μPAD fabricated by photolithography was enhanced by the oxygen plasma treatment, and thus performance became the same as for the wax-printed μPAD. These results indicate the fabrication methods affected the wicking property of μPADs and their performance could be improved by selecting suitable fabrication methods, post treatment, and experimental conditions.

Comparison of performance for protein assay using the μPADs

Finally, we compared the performance for the protein assay using the μPADs. We carried out the colorimetric protein assay in triplicate, and compared the μPADs using the K-scale (color scale)[29] and standard deviation (STD) of color scale. Figure 3(a) shows photographs of μPADs used for the colorimetry.

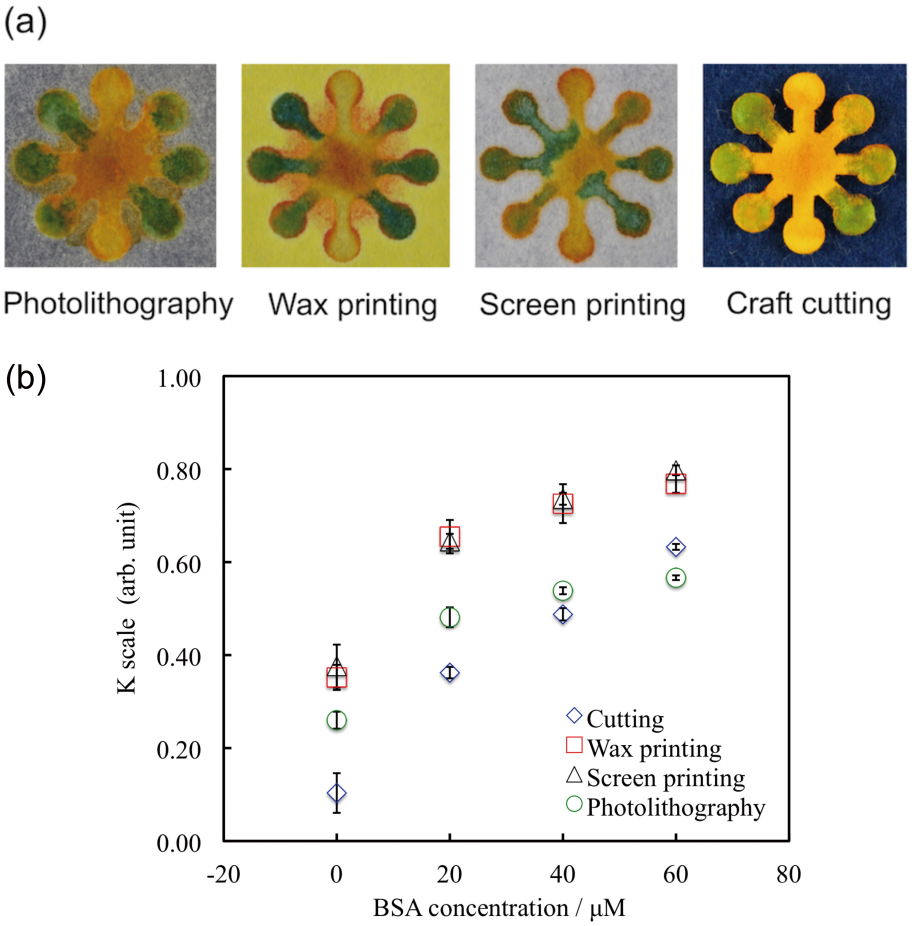

Fig. 3 Protein assay using the μPADs fabricated by four methods: (a) photographs of the μPADs for colorimetric analysis. (b) The calibration plot of the protein assay using the four μPADs.

The protein reacted with TBPB to give detection zones with a blue color. Figure 3(b) presents the calibration plot of the protein assay using the μPADs. The K-scale of the μPAD fabricated by craft cutting was lower than the values of the other μPADs. We consider that the evaporation rate of the craft cut μPAD was higher than those of the other μPADs, because the solution could evaporate not only from the top and back sides of the device, but also from the edges. BSA molecules (66 kDa) cannot diffuse into all of the detection zones due to the rapid evaporation of the solvent. The diffusion or transfer rate of protein molecules depends on the drying condition of the paper substrate, and might be limited, even with the semi-dried condition due to rapid evaporation. In other words, all the BSA molecules introduced into the detection zones could not react with TBPB. For this reason, the color intensity obtained from the craft cut μPAD was low. The K-scale of the μPAD fabricated by photolithography also showed lower intensity compared with the two types of printing-based μPADs. The introduced solution could not flow homogeneously into the μPAD fabricated by photolithography, because of the leakage of solution from the introduction zone and the shortage of hydrophilic cellulose fibers inside the paper substrate by a plasma treatment of all the total topside area of the μPAD. Therefore, BSA diffused non-uniformly and did not react with TBPB in the detection zones. On the other hand, the K-scale values of the μPADs fabricated by wax printing and screen printing were of higher intensity than those of the other μPADs. The hydrophilic area of printing-based μPADs are composed of bare cellulose fibers, and the solution can only evaporate at the top and back sides of the paper substrates. We consider that the bare cellulose fibers and desirable diffusion rate of proteins were responsible for the high detection intensity. However, we did not confirm any large difference in the STD among the μPADs, because of the similar color reproducibility in detection zones among the μPADs. We fabricated three μPADs for each fabrication method, and carried out the protein assay three times. This result indicates that the assay reproducibility of the μPADs fabrication and of the protein assay was confirmed, regardless of the fabrication methods.

Conclusions

We investigated the characteristics of μPADs fabricated by four different methods: photolithography, wax printing, screen printing, and craft cutting. Photolithography has complicated fabrication procedures, and an oxygen plasma treatment is necessary to introduce an aqueous solution into the μPAD. The boundary between the hydrophobic and hydrophilic areas was formed most sharply for the photolithography method among the four methods. However, the K-scale intensity of this device was lower than those of the other devices. Wax printing offers a simple and rapid fabrication, although the leakage of the solution should be prevented to improve the wicking rate and to avoid cross-contamination. Screen printing is also an easy fabrication method. The screen-printed μPAD had a good wicking property and showed high detection intensity.

Craft cutting provides an automated fabrication for many μPADs at once. The craft cut μPAD had the fastest wicking rate among the four μPADs due to the bare cellulose fibers. In conclusion, our reports established that different hydrophobic barrier conditions due to different four fabrication methods effected to the analytical properties, such as the wicking rate and the evaporation rate. We assume that the detection intensity can be raised by optimizing the evaporation rate. Therefore, we believe that these reported characteristics of the μPADs will promote development of other new μPADs and will lead to improved μPAD performance.

Acknowledgements

This research was supported by the Urakami Foundation for Food and Food Culture Promotion. We acknowledge JASCO International Co., Ltd., for taking SEM images. T. K. thanks the Ambitious Leaders' Program for Fostering Future Leaders to Open New Frontiers in Materials Science.

Supporting Information

This material is available free of charge on the Web at http://www.jsac.or.jp/analsci/.

References

1. Y. Yang, E. Noviana, M. P. Nguyen, B. J. Geiss, D. S. Dandy, and C. S. Henry, *Anal. Chem.*, **2017**, *89*, 71.
2. L. S. A. Busa, S. Mohammadi, M. Maeki, A. Ishida, H. Tani, and M. Tokeshi, *Micromachines*, **2016**, *7*, 86.
3. D. Cheng, X. Zhang, X. Li, L. Hou, and C. Wang, *Anal. Sci.*, **2017**, *33*, 185.
4. N. A. Meredith, C. Quinn, D. M. Cate, T. H. Reilly, J. Volckens, and C. S. Henry, *Talanta*, **2016**, *141*, 1847.
5. L. H. Mujawar, A. A. Felemban, and M. S. El-Shahawa, *Anal. Sci.*, **2016**, *32*, 491.
6. L. Syedmoradi, M. Daneshpour, M. Alvandipour, F. A. Gomez, H. Hajghassem, and K. Omidfar, *Biosens. Bioelectron.*, **2016**, *86*, 353.
7. F. Hori, Y. Harada, T. Kuretake and S. Uno, *Anal. Sci.*, **2016**, *32*, 355.
8. J. Sittiwong and F. Unob, *Anal. Sci.*, **2016**, *32*, 639.
9. K. Tominaga, S. Arimoto, K. Shimono, T. Yoshioka, F. Mizutani, and T. Yasukawa, *Anal. Sci.*, **2017**, *33*, 531.
10. A. W. Martinez, S. T. Philips, M. J. Butte, and G. M. Whitesides, *Angew. Chem. Int. Ed.*, **2007**, *46*, 1318.
11. A. W. Martinez, S. T. Phillips, G. M. Whitesides, and E. Carrilho, *Anal. Chem.*, **2010**, *82*, 3.
12. L. S. A. Busa, T. Komatsu, S. Mohammadi, M. Maeki, A. Ishida, H. Tani, and M. Tokeshi, *Anal. Sci.*, **2016**, *32*, 815.
13. E. Carrilho, A. W. Martinez, and G. M. Whitesides, *Anal. Chem.*, **2009**, *81*, 7091.
14. K. Ogawa and T. Kaneta, *Anal. Sci.*, **2016**, *32*, 31.
15. K. Abe, K. Suzuki, and D. Citterio, *Anal. Chem.*, **2008**, *80*, 6928.
16. X. Li, J. Tian, and W. Shen, *Cellulose*, **2010**, *17*, 649.
17. J. L. Delaney, C. F. Hogan, J. Tain, and W. Shen, *Anal. Chem.*, **2011**, *83*, 1300.
18. X. Yan, Y. Zheng, J. Gao, and J. Lee, *Anal. Sci.*, **2017**, *33*, 1.
19. S. Mohammadi, M. Maeki, R. M. Mohamadi, A. Ishida, H. Tani, and M. Tokeshi, *Analyst*, **2015**, *140*, 6493.
20. W. Dungchai, O. Chailapakul, and C. S. Henry, *Anal. Chem.*, **2009**, *81*, 5821.
21. Y. Sameenoi, P. N. Nongkai, S. Nouanthavong, C. S. Henry, and D. Nacapricha, *Analyst*, **2014**, *139*, 6580.
22. J.-Y. Sun, C.-M. Cheng, and Y.-C. Liao, *Anal. Sci.*, **2015**, *31*, 145.
23. W. Liu, Y. Guo, M. Zhao, H. Li, and Z. Zhang, *Anal. Chem.*, **2015**, *87*, 7951.
24. J. Yu, S. Wang, L. Ge, and S. Ge, *Biosens. Bioelectron.*, **2011**, *26*, 3284.
25. P. K. Yuen, and V. N. Goral, *Lab Chip*, **2010**, *10*, 384.
26. X. Li, D. R. Ballerini, and W. Shen, *Biomicrofluidics*, **2012**, *6*, 011301.
27. A. K. Yetisen, M. S. Akram, and C. R. Lowe, *Lab Chip*, **2013**, *13*, 2210.
28. L. S. A. Busa, M. Maeki, A. Ishida, H. Tani, and M. Tokeshi, *Sens. Actuators, B*, **2016**, *236*, 433.
29. T. Komatsu, S. Mohammadi, L. S. A. Busa, M. Maeki, A. Ishida, H. Tani, and M. Tokeshi, *Analyst*, **2016**, *141*, 6507.